#631 To [illegible] meeting in GA. USA. 6-8 Aug. 92

631

Fabrication and Optical Properties of Rare-Earth doped Lead-Germanate Glasses and Fibres

J. Wang, J.R. Lincoln#, R.S. Deol, W.S. Brocklesby# and D.N. Payne

Optoelectronics Research Centre and
Department of Physics#
University of Southampton
Southampton SO9 5NH
United Kingdom

Tel: +44 703 593172
Fax: +44 703 593149

Abstract

A lower maximum phonon-energy lead-germanate glass suitable for fibre optic-applications has been achieved by optimizing the glass composition via the Levin-Block concept. Some cladding silicate glasses compatible with the optimized core-glass are identified. These lead to the realization of a new class of rare-earth doped, low-loss, high strength as well as low cost, multicomponent glass optical fibres for fibre device applications. Absorption and emission spectra, together with fluorescent decay times for Tm^{3+} ions in the glass are present. The reduced maximum phonon-energy of lead-germanates (890 cm^{-1}) over that of silicates (1150 cm^{-1}) leads to an extension of the metastable lifetimes in Tm^{3+}. The role of Pb^{2+} in influencing the glass structures and properties is also addressed.

1. Introduction

Rare-earth doped optical fibres have received considerable attention in recent years due to the enhanced performance that optically pumped fibre devices can give over bulk glass devices. The major advantage of fibre technology is the guiding, and therefore confinement of light, which can increase the interaction volume of the pump light with the active medium while maintaining high light intensities [1]. The principle limiting factor on the number of devices which have been demonstrated in optical fibre structures has been the very small number of glasses that have been fabricated into the low loss optical fibre necessary for efficient device performance. For many years low loss fibre fabrication has been confined to silica or modified silica glasses, although in the last a few years fluoride-based ZBLAN glass fibres have also become available. We see it as absolutely essential that the range of rare-earth doped glasses that can be made into fibre structures is extended, particularly into lower phonon-energy glasses combining possibly the best properties of both silica (low-loss, high strength etc.) and fluoride-based glasses (low non-radiative relaxation rate, etc.).

In this paper, we report the preparation and characterisation of Tm^{3+}-doped lead-germanate based glasses and fibres. Fabrication of a lead-germanate glass suitable for fibre optic applications is successfully achieved by optimizing the glass composition using the Levin-Block concept developed in late 1960's [2,3,4]. The optimized lead germanate glass shows a remarkable thermal-stability characteristic, exhibiting no devitrification phenomenon throughout the entire temperature range from T_g to T_m. Particular silicate glasses which are both thermally and optically compatible with the ultimately optimized lead-germanate core-glass are identified as suitable cladding materials. These lead to the realization of a new class of rare-earth doped, low loss, high strength as well as low cost, multicomponent-glass optical fibres suitable for fibre device applications, by a simple, flexible conventional rod-in-tube technique.

Raman spectra of a range of lead-germanate based glasses confirm that the maximum phonon-energy of these glasses is intermediate between those of silica and fluoride-based glasses. The lower frequency shift of the maximum phonon-energy peaks in the Raman spectra of lead-germanates compared to that of pure germania glass is examined and interpreted with respect to the role of Pb^{2+} in the glasses.

Absorption and emission spectra, together with electronic level decay times for Tm^{3+}-doped lead-germanate provide an extensive characterization of the optical properties of this rare-earth ion in the lead-germanate host. The reduced maximum phonon-energy of lead-germanates (890 cm^{-1}) over that of silicates (1150 cm^{-1}) produces a substantial gain in extending the metastable level lifetimes in Tm^{3+}, as expected with the prediction from the multiphonon decay mechanism. On the other hand, the maintenance of the maximum phonon-energy above that found in fluoride-based ZBLAN (580 cm^{-1}) enables multiphonon emission to be utilised with high efficiency in populating the upper level of Tm^{3+} $^3H_4 \rightarrow {}^3H_6$ transition. This enhances the performance of lasing this $^3H_4 \rightarrow {}^3H_6$ transition at around 2μm with a laser diode compatible pumping scheme [5] by exciting the Tm^{3+} $^3F_4$ level at a wavelength around 790nm. Improvements in the 2μm fibre laser performance in a lead-germanate fibre host compared to those in silica and fluoride-based ZBLAN, glass fibre hosts are noted and have been reported earlier [6]. Comparison of the optical properties of Tm^{3+}-doped germania and various modified lead-germanates confirms the dominant role of Pb^{2+} in the latter in influencing the glass structure and properties. The variation in the lifetimes of Tm^{3+} electronic levels between different bulk lead-germanates and lead-germanate fibre is also addressed.

2. Experimentals

Glass Preparation

Glasses were prepared from anhydrous oxide powders for Ge, Al, Zn, Pb and Tm, and anhydrous carbonate powders for Ba, Ca and K. All chemicals were of common analytical grade except for GeO_2 which was of electronic grade (99.999% purity, Aldrich), and Tm_2O_3 which was of 99.9% purity (Aldrich). Glass batches, in quantities of 150-200g of powder, were mixed for at least half an hour in a cleaned glass container mounted on a rotating lathe. Batches were then melted in a platinum crucible placed in an electrically-heated furnace, containing an air atmosphere, at temperatures between 1000°C and 1250°C, depending on the glass. The melts were kept well stirred with a silica rod to achieve homogeneous mixing possible, and later refined to remove bubbles. The refined glass-melts were removed from the furnace at 1150°C and cast into a prewarmed stainless steel mould before being annealed in a muffle furnace at around 500°C. All glasses contained 0.5 wt.% Tm_2O_3 as an active dopant. A series of smaller undoped

samples, prepared from 20g of powdered constituents were also made for the thermal treatment tests, using a similar temperature arrangement to the larger samples. Homogeneity was achieved in the smaller samples by shaking, rather than stirring, the melts in the crucible at 1200°C.

Thermal Analysis

Thermal analysis of the glasses was carried out on a commercial Netzsch 404 type differential scanning calorimeter (DSC). Typically about 50mg powdered samples were heated at a rate of 20°C per minute, from room temperature to 1100°C in an air atmosphere. The crucibles used were matched pairs made of alumina, and the temperature precision was ± 0.1°C. The thermal stability of the bulk lead-germanate glasses was also tested by placing samples in a muffle furnace heated to the likely fibre pulling temperatures, around 750°C, and then holding the samples at that temperature in the furnace for at least half an hour to assess their crystallization tendencies.

Spectroscopy

Raman spectra were recorded using a commercial triple grating spectrometer equipped with a nitrogen cooled CCD detector. Bulk glass samples were excited with an argon ion laser at either 514.5nm or 488nm and the Raman signal recorded in a 180° backscattering geometry. No polarisation selection was used in detection.

Absorption spectra were recorded from polished bulk glass samples on a white light spectrophotometer (Perkin-Elmer Lambda 9) with automatic correction for detector response. Visible fluorescence spectra and decay times were measured by exciting samples with either an Argon ion laser or an Argon pumped Pyrenene 2 dye laser. The excitation beam was chopped with an acousto-optic modulator and the pump light focused onto the bulk sample or into the core of the optical fibre. Fluorescence was monitored from light scattered out of the side of fibres, or from close to the surface of bulk samples. Emission spectra were recorded on a 1 metre spectrometer, equipped with a flat response, photon counting, GaAs photomultiplier tube. Lifetimes, of visible fluorescence, were taken using the same apparatus and using the photon counter as a box car averager. Infrared fluorescence spectra were recorded using a scanning 0.3m spectrometer and PbS photodiode detector. Infrared lifetimes were recorded using a nitrogen cooled InAs photodetector and germanium filters to block the visible light. Decay lifetimes were derived by fitting a single exponential decay function to the

observed fluorescence decay using a statistically weighted non-linear least squares fit routine.

3. Fabrication of a Lead-Germanate Glass Suitable for Fibre Optic Applications

Initial trials

Glasses based on germanium dioxide have long been known to have better IR transmission than glasses based on silicon dioxide, extending in some cases up to 5.5μm [7]. This extended IR transmission is due to the larger size and the heavier mass of germanium when compared to silicon. The Ge^{4+} is therefore more weakly bonded to the surrounding O^{2-} ions and the associated bonds have lower vibrational frequencies and energies than similar Si-O bonds. The weaker bonding also means glasses based on GeO_2 have smaller stable glass formation ranges than glasses based on SiO_2 [8]. The manufacture of multicomponent germanate glasses, without devitrification, is therefore harder than similar silica based systems, and may require more rapid quenching rates. Pure GeO_2 glass and germania-rich glasses are also known to have a tendency to react with atomospheric moisture [9], again undesirable for high grade optical fibres.

It has been previously reported that a series of lead-germanate based ternary glass systems have relatively large glass forming regions, compared to other germanate systems, whilst maintaining high infrared transmission [10]. Among these, a specific glass of the composition $63GeO_2$-27PbO-10CaO (in mole percentage) was also noted to have inherently less OH^- contamination. Therefore, a lead germanate glass with initial composition $63GeO_2$-27PbO-10CaO was fabricated at 1050°C in air, to be evaluated for fibre fabrication. The resulting glass, made from this composition, was found to be stable by the conventional casting procedure, and no devitrification either on surface or in volume form was observed for the bulk materials. The fibre pulling temperature, corresponding to viscosity, η, of about 10^5 poise, for this glass was estimated as 50-100°C above T_s, where $\eta=10^{7.6}$ poise. The value of T_s was obtained from the two third rule [11], an empirical relationship between T_g and T_s, resulting in a fibre pulling temperature range of 700°C to 750°C. However, as shown in Fig. 1a, devitrification occurred in the hot zone of the fibre pulling furnace when attempting to pull this glass into a fibre at temperatures around 700°C - 750°C. The DSC measurement of this initial glass, presented in Fig. 2, clearly shows two exothermic peaks at around 710°C and 750°C

respectively, indicating strong crystallisation at these temperatures. The severe crystallisation of this $63GeO_2$-27PbO-10CaO glass in the fibre pulling temperature range made this composition useless for its fibre optic applications.

In order to further stabilize the glass up to 10 mol% aluminium oxide, Al_2O_3, was added to the initial glass composition, since it is known [12] that alumina is effective in stabilizing some silicate glass melts by acting as additional linkages for the three dimensional glass framework that is partially broken by the glass modifiers. Following preparation of a series of modified lead germanate glasses with compositions

$$63GeO_2\text{-}27PbO\text{-}10CaO\text{-}xAl_2O_3,\ x = 1, 2, 5, \text{ and } 10$$

at 1150-1250°C, thermal tests of the glasses in a muffle furnace at 750°C for 30 minutes showed that all samples devitrified. The DSC measurements were also conducted and the results for the sample x = 5 is shown in Fig. 3. It can be seen from Fig. 3 that the exothermic peak indicating crystallisation at 710°C that was observed in the original $63GeO_2$-27PbO-10CaO glass, Fig. 2, has been eliminated on the addition of alumina. However, the more severe exotherm-crystallization peak at 750°C was still present, Fig. 3, despite the addition of alumina. The substitution of CaO by BaO was also made in above system. However, thermal treatment tests at 750°C in a muffle furnace showed similar devitrification features to the CaO containing glasses. It was therefore concluded that alumina is not a sufficiently efficient intermediate-component in the lead-germanate glass system to provide the high-temperature glass stability which is crucial for fibre fabrication. Hence, another, more effective, intermediate-component must be established to impart high temperature stability to the lead-germanate glasses.

The Levin-Block Concept

Levin and Block, in the 1960's [2, 3, 4], have systematically studied the immiscibility phenomenon in oxide glass systems by applying the principles of crystal chemistry. They concluded that the occurrence of immiscibility in a glass was purely governed by the bond strengths of the modifying and the intermediate cationic ions involved in the glass. To quantify the bond strength, they used the ionic field strength (IFS) defined as

$$\text{IFS} = \frac{Z}{(R^+ + 1.40)^2} \qquad (1)$$

where Z is the charge on the cation and the $(R^+ + 1.40)$ term is the interatomic

separation, taken as the sum of the cationic radius and the oxygen ionic radius. It was suggested that the extra phases would not occur if the modifying or intermediate cation-oxygen field strengths were either too strong or too weak relative to the corresponding strength of glass former in the system. Quantitatively, a system would remain in a single phase if the difference in ionic field strengths between the glass former and the modifier (ΔIFS) was greater than 0.8 or less than 0.06 [4, 13]. For the case of an intermediate component, the actual figures were not given, however the similar principle should be followed. We believe that the Levin-Block principle can also be applied to the crystallization, as well as to the glass phase separation, since the occurrence of extra phases either in glass or in crystal form is a matter of where the glass composition is situated in the specific phase diagram. Although the Levin-Block concept has been criticized for its ignoring the influence of temperature [14], it has been found appropriate for most of the oxide systems, including the germanate systems [4, 13], therefore we propose it should provide as a general basic guidance for the optimization of glass compositions.

Optimizing the Composition Suitable for Fibre Fabrication

It is known that the basic germanate glass structural unit, consisting of germanium-oxygen GeO_4 tetrahedra, has a larger volume than the SiO_4 tetrahedra found in silicate glasses, with a Ge-O bond distance of 1.74Å in pure GeO_2 glass in contrast to a Si-O bond distance of 1.60Å in silica [15]. The corresponding ionic field strengths (IFS) for Ge-O and Si-O bonds are 1.074 and 1.208 respectively [13]. According to the Levin-Block concept, in order to maintain the difference of IFS between the glass former and the modifier within the same required limits, the modifiers required by germanate glass should have lower IFS values than those required by silicate glass. From equation (1), this means that a larger modifying ion size is demanded for the stable formation of germanate glasses, compared to the formation of silicate glass, if the same charged ions are used. A similar trend should also be followed by the intermediate ions.

For the germanate glasses we utilized ZnO as an intermediate element instead of Al_2O_3, since Zn^{2+} has an ionic radius, $R_{Zn^{2+}}$, of 0.74Å [13] much larger than the ionic radius of Al^{3+}, $R_{Al^{3+}}$=0.51Å [13]. More importantly, it can be noted that Zn-O bond possesses a ΔIFS of about 0.6 relative to Ge-O compared with only 0.25 for Al-O relative to Ge-O [13]. The latter can be contrasted to the Al-O bond relative to Si-O, which has a ΔIFS of about 0.4 [13]. We believe that it is the insufficient difference in IFS for

alumina in germanate that accounts for its weakness as an effective intermediate component. For the modifier component, according to the Levin-Block concept, barium oxide, BaO, was found to be more suitable than CaO. Barium oxide, $R_{Ba^{2+}}$=1.34Å [13], has a ΔIFS value of 0.81 relative to Ge-O, just above the critical value of 0.8, whilst calcium oxide CaO, $R_{Ca^{2+}}$=0.99 Å [13], has a ΔIFS value of 0.72 relative to Ge-O less than the required 0.8. To further ensure ZnO acted as the intermediate component, potassium oxide K_2O ($R_{K^{1+}}$ = 1.33 Å, ΔIFS = 0.94 > 0.8 relative to Ge-O [13]) was also added to the composition as a modifier providing extra free O^{-2} ions required for the possible formation of ZnO_4 tetrahedral units in the glass network [16].

In order to make a proper estimation of the amount of each ingredient in the glass, the following two points were considered. First, the ratio of GeO_2/PbO was required to be near 3, because the phase diagram of the GeO_2-PbO binary system exhibits crystal compounds at GeO_2/PbO ratios of both 2 and 4 [17]. For a stable glass formation, it was desirable to be as far from these points as possible. Secondly, the ratio of R_2O(RO)/ZnO need to be much grater than unity, to ensure the formation of ZnO_4 [16]. Consequently, the following glass compositions were designed:

(a) $55GeO_2$-20PbO-10CaO-10ZnO-$5K_2O$

(b) $55GeO_2$-20PbO-10BaO-10ZnO-$5K_2O$

Composition (a), with CaO still as modifier, was fabricated to test the Levin-Block concept. The thermal treatment tests carried out at 750°C in a muffle furnace for the two glasses prepared from the above compositions showed that as anticipated glass (a) crystallized, but glass (b) exhibited no crystallization. The DSC measurements of the two glasses are shown in the upper and lower halves of Fig. 4. For glass (a) a similiar crystallization, exotherm, peak can be seen similar to those exhibited by the previous glass samples although it appears at the slightly lower temperature of 746 °C, instead of 755 °C. From the lower part of Fig. 4 it can be seen that Glass (b) shows no exotherm peaks, and therefore no crystallization, over the entire temperature range from T_g to T_m. Glass of composition (b), now abbreviated to GPBZK, is therefore extremely stable and was chosen as for fibering purposes.

Further examination of the DSC curve of glass (b), shown in the lower part of Fig. 4, gave values for T_g of about 465°C, T_s of about 665°C and T_m of about 922°C for this glass. These were determined by the intersects between the base line and the starting edges of the respective small endothermic-humps in the DSC curve [18], as shown in Fig.4. Caning of glass rod of composition (b), in a fibre pulling furnace, was successfully

performed at about 700 °C, as shown in Fig. 1b.

The above results illustrate the usefulness of the Levin-Block concept in optimizing the glass compositions. To our knowledge, this has been the first time the Levin-Block concept being utilised in this way for the optimization of composition for stable glass formation.

4. Cladding Glasses and Fibre Manufacturing

Cladding Glasses

In order to fabricate our optimized lead germanate glass into an optical fibre structure, a suitable cladding glass had to be found with compatible optical, thermal and chemical properties to our core glass. The most obvious cladding glass to use is one with a composition slightly amended from the core glass composition in a way that reduces the refractive index by a small fraction. However, this approach was not implemented in this research due to its very expensive cost of the large amounts of high grade GeO_2 raw materials required to make a modified lead-germanate cladding. Instead, the commercial Schott SF series lead-silicate glasses were considered as possible candidates for cladding materials because their optical, thermal and chemical properties might be matched to our lead-germanate core-glass. Also, these glasses could be acquired with a guaranteed high optical quality together with detailed information on their optical, chemical and thermal properties.

The major difficulty in selecting a suitable clad from the lead-silicate glasses, which have such a fundamentally different composition to our core glass, is in matching the viscosities of the cladding and the core glasses at the fibre pulling temperature. At the same time the cladding glass must also possess the desirable refractive index, matched thermal expansion coefficient etc. to the core-glass. Matching the T_g and T_s between the clad and the core, as we had been reported for the lead-silicate glass fibres [19], is no long relevant, because the core and the clad belong to two distinctively different glass systems and have different viscosity temperature dependencies. Although, it is well known that the viscosity, η, varies with temperature, T, according to the following Arrhenius-type expression [20]:

$$\eta = \eta_0 \exp\left(\frac{E}{RT}\right) \qquad (2)$$

where η_0 is a temperature-independent constant and E is the activation energy. It has been found [21] that the activation energy E decreases with increasing temperature, which makes the use of Equ. (2) for the theoretical prediction of the fibre pulling temperature range (corresponding to the viscosity of about 10^5 poise for rod-in-tube technique [18]) extremely difficult. Therefore, the only accurate method for determining the fibre pulling temperature of the possible cladding glasses is to try the glasses experimentally using its glass-rod in the fibre pulling furnace to define the fibering temperature range. Of the Schott glasses tried, SF16 and SF56 were both found to have a similar fibering temperature range to the core glass, at around 700 °C.

To finally assess the suitability of SF16 and SF56 as cladding glasses it was necessary to compare the thermal expansion coefficients and refractive indices to the lead-germanate core-glass. The refractive index, n_D, and the thermal expansion coefficient, α, of the lead-germanate core glass were calculated using the Gan's method [16] to be 1.804 and 118.8×10^{-7} °C^{-1} respectively (The error in this type of calculation was about $\pm 7 \times 10^{-3}$ for the refractive index and $\pm 6 \times 10^{-7}$°C^{-1} for thermal expansion coefficient [16]). The refractive index of the core glass was measured experimentally by the prism coupling method [22] and found to be 1.812 ± 0.005 in reasonable agreement with the calculated figure. An experimental value for thermal expansion coefficient, α, was not available. Compared the refractive index and thermal expansion coefficient of the core-glass with those of the SF16 (n_D of 1.646 and α of 93×10^{-7} °C^{-1}) and the SF56 (n_D of 1.784 and α of 88×10^{-7} °C^{-1}), it was confirmed that both of these cladding glasses would provide a guiding structure for optical fibres and both cladding glasses were also having well matched thermal expansion coefficients to that of the lead-germanate core glass ($\Delta\alpha < 50 \times 10^{-7}$ °C^{-1} [23]) .

Fibre Fabrication

The fibre fabrication was performed by the rod-in-tube technology [19]. The core and cladding were drilled out from the corresponding bulk glasses with an ultrasonic drilling machine. The ultrasonically cleaned lead-germanate core-glass rod (10 mm in diameter) was further caned into 1 to 2 mm in diameter in the fibre drawing furnace, with a hot

zone of 20mm in length x 20mm in diameter, to ensure a fire polished smooth surface ready for use as the fibre core. The cladding-glass rod with an appropriate drilled hole area in the middle could either be priorly chemically polished using 5% HF solution for about 15-30 seconds, or be used directly after thorough cleaning without chemical polishing to form the rod-in-tube combination. As shown in Fig. 1c, the non-prior etched cladding was able to be fire polished in the hot zone of fibre pulling furnace just before the fibre was drawn at around 700°C.

Fig. 5 shows the cross section of optical fibre drawn with the combination of the optimized lead-germanate as core and the Schott SF56 lead-silicate as cladding by the rod-in-tube technique. A fine, clean and well defined core-clad interface can be clearly seen, showing good chemical compatibility between these two different types of glasses at the fibre pulling temperature range. The mechanical strength of the fibres was also good displaying a bending radius of 5 mm possible in uncoated fibre, which is comparable with the bending radius obtainable in bare silica fibres. Fibres have been pulled with 3-10 μm core diameters and more than 50 meters in lengths, with either SF56 or SF16 as a cladding. The background fibre loss was typically 2 dB/m and probably represents the background loss of the bulk glass used in the fibre core, which was limited by the purity of the starting materials or the manufactural conditions, with minimal losses therefore attributable to imperfections in the fibre.

5. Spectroscopic characterisation

Vibrational Spectroscopy

Raman spectra of the bulk lead germanate glass, $55GeO_2$-20PbO-10BaO-10ZnO-$5K_2O$:Tm_2O_3, used in the fibre core and an 'in house' melted pure germanate glass are presented in the upper and lower halves of Fig. 6. Full Raman spectra from 200-1400cm^{-1} are shown for 514.5nm Ar^+ ion laser excitation and the insert shows the Raman spectra of the GPBZK glass above 600cm^{-1} excited with the 488nm Ar^+ line.

The Raman spectra of the pure GeO_2 agrees with similar results previously reported by F.L. Galeener et al [24]. The spectra given in the upper half of Fig. 6 for the GPBZK given are complicated by the presence of erbium contamination in the GPBZK glass. The peaks in the 514.5nm excited Raman spectra, marked '*' in Fig. 6, can be attributed to erbium fluorescence on the Er^{3+} $^4S_{13/2}$-$^4I_{15/2}$ and Er^{3+} $^2H_{11/2}$-$^4I_{15/2}$ transitions. This is confirmed for the peak at over 1200cm^{-1} (=550nm) by it's

disappearance from the Raman spectra excited at 488nm. However, a similar confirmation of the Raman peaks below 600cm^{-1} was not possible, due to fluorescence from the $^1G_4$ level of the thulium doped into the glass dominating Raman scattering at frequencies below 600cm^{-1}, relative to 488nm. The source of the erbium contamination of the GPBZK glass has been confirmed, due to its presence in the original thulium oxide.

The Raman spectra of the other bulk lead germanates fabricated with compositions CaO-PbO-GeO_2 and CaO-PbO-Al_2O_3-GeO_2 were also recorded and appeared almost identical to the spectra given in the upper half of Fig. 6 for the GPBZK glass. Small shifts, <20cm^{-1}, in the position of the highest energy phonon peak were observed, but could not be definitely attributed to peak shifts in the Raman lines due to the problems of erbium contamination.

The drastic change in the Raman spectra from pure germanate, lower spectra Fig. 6, to lead germanates, upper spectrum Fig 6, can be attributed to the effect of the lead on the GeO_2 glass structure. It has been postulated by H.Hagiwara et al [25] that Pb^{2+} distorts, but does not destroy, the tetrahedral GeO_4 network in the lead germanate glass. It is suggested that Pb^{2+} breaks some of the bridging oxygen bonds in the glass which join the Ge^{4+} ions. The very strong covalent nature of the lead with the oxygen distorting and loosening the GeO_4 tetrahedra and hence reducing the frequency of the anti-symmetric stretching vibrations of the GeO_4 tetrahedra, by weakening the Ge-O bonds. If the highest energy phonon peaks observed in the Fig. 6 are attributed to these anti-symmetric stretching vibrations then the observed shift to lower energy of these vibrations is consistent with the strong covalent interaction of the lead with the oxygen ions.

Our interest in the maximum phonon energy of the glasses in question lies in the effect of the phonon energy on the multiphonon decay rate. Theories of multiphonon decay are generally based on the maximum peak phonon energy, rather than the shape of the vibrational spectrum, and so do not take into account whether the highest-energy peak is narrow or broad[26]. This is reasonable in crystal hosts, where sharp peaks occur in the vibrational density of states, however in a glass like lead-germanate there can be a large difference between the highest-energy peak and the highest energy at which a sizeable density of states still exists. In order to make a reasonable estimate of the contribution of the peak width, we have chosen to define our maximum vibrational energy as the point at which the density of states is reduced to 1/e, i.e. 36.8%, of the maximum peak height. This definition yields maximum vibrational energies higher than

those given by measuring the peak positions, but we believe that it is necessary to take into account peak widths. The maximum vibrational energies, measured on this basis, are: ZBLAN 620cm^{-1} (580cm^{-1}), aluminosilicate glass 1250cm^{-1} (1150cm^{-1}), GeO_2 glass 1040cm^{-1} (980cm^{-1}), and GPBZK glass 890cm^{-1} (820cm^{-1}). The values in the brackets are the highest peak phonon-energies respectively. From these figures for the maximum phonon energy it is clear that we have achieved a fibre compatible host glass with maximum phonon energy intermediate between silica and fluorzirconates.

Absorption

The absorption cross-section derived from 0.5 wt% doped GPBZK glass is presented in Fig. 7. Energy level assignments for the various thulium absorption bands are also given above the absorption peaks. Absorption data was recorded from a polished slab of bulk glass, taken from the same melt batch used to fabricate the final fibre core. The value of the absorption cross-section was calculated from the white light absorption in dBm^{-1} using a glass density of 5.7g/cm^3, measured by the Archimedes method, and a Tm_2O_3 concentration of 0.5 wt%, equivalent to 8.7x10^{19} ions.cm^{-3}. The assignment of the energy levels, in particular the $^3F_4$ and $^3H_4$ bands, follows the zero spin orbit coupling convention [27].

The positions of the absorption peaks, shown in Fig. 7, for the GPBZK glass are very similar to thulium doped fluorzirconbate based glass, eg ZBA [28], and are therefore shifted slightly from thulium silicates [29]. The spectral width of the absorption bands for Tm^{3+} in PKBZG is intermediate between Tm^{3+}:fluorzirconates and Tm^{3+}:silicates. From the spectra it can seen that the absorption into both the $^3H_4$ and the $^1G_4$ levels has a double peak structure, unseen in either fluorzirconate based or silica based thulium hosts, indicating a rather well-defined local environments around Tm^{3+} in the PKBZG glass.

Fluorescence Decay

Given in Fig. 8 are the fluorescent decay lifetimes for the $^1G_4$, $^3F_4$ and $^3H_4$ levels of thulium doped into pure GeO_2, CaO-PbO-GeO_2, CaO-PbO-Al_2O_3-GeO_2 and 55GeO_2-20PbO-10BaO-10ZnO-5K_2O bulk glasses and the initial GPBZK fibre. The fluorescent decay from the $^1G_4$ level was well represented by a single exponential decay function. Single exponentials did not fit perfectly to the $^3F_4$ fluorescence decays, but the results of these fits will be used here to give a reasonable estimation of the $^3F_4$ lifetime.

Explanations for the non-exponential behaviour of the $^3F_4$ fluorescence decay in thulium have been given previously by J.R.Lincoln et al [29]. The quality of the single exponential fits to the $^3H_4$ decays was harder to asseses due to the smaller dynamic range of fluorescence decay recorded. The $^3H_4$ lifetime for $CaO\text{-}PbO\text{-}Al_2O_3\text{-}GeO_2$ was not recorded.

The values for all $^3H_4$ lifetimes given in Fig. 8 are all substantially longer than the 500 μsec lifetime measured for thulium in alumino-silicates [30]. This reflects the substantial decrease in the maximum phonon energies for the germanate glasses, in comparison to the silicate based glasses, noted from the Raman spectra. The observed $^3H_4$ lifetime for the pure thulium germanate, given as 2.27msec in Fig 8, correlates with the predictions of Reisfeld et al [31] which gave a predicted decay time of 3msec for this level. From Fig. 8, it can also be clearly seen that, in the thulium doped modified lead germanates, the $^3H_4$ Tm^{3+} lifetime has been further extended from the value in pure GeO_2 glass. This change in lifetime is consistent with the lowering of the maximum phonon energy of the modified lead-germanates in comparison to pure germanates, as noted above.

The final $^3H_4$ lifetime given in Fig. 8 for GPBZK fibre shows a substantial shortening of the $^3H_4$ lifetime from bulk glass to fibre of 3.16msec to 2.35 msec. The reasons for this drastic shortening in the lifetime are at present unclear. It is possible that this lifetime is quenched by energy transfer to defects in the fibre, with a higher number of these present in the fibre induced by intense quenching in the fibre drawing process. Similar lifetime shortening effects have also been seen for other thulium levels when comparing silica-based fibres and their preforms [29] and have been attributed to cross-relaxation mechanisms, which are more apparent in fibres because of the higher excitation intensities. The probability of cross-relaxation occurring in the GPBZK glass is high due to the high thulium concentration of $8.7x10^{19}$ ions.cm^{-3}. This concentration is equivalent to a Tm^{3+} ion separation of about 22.5Å (assuming a homogenous dopant distribution). This ion separation is close to the critical ion separation for efficient energy transfer, reported to be around 20Å [32]. Cross-relaxation has also been recorded at Tm^{3+} ion average-separation of 35Å in fluorzirconate based glasses [28]. Clustering of the thulium ions was suggested in these glasses. It is likely that the Tm^{3+} clustering effect also presents in the lead-germanate host. Finally, it is also possible that the high excitation intensities in the fibre build up sufficient population inversion in the $^3H_4$ level for amplified spontaneous emission to occur from the level to become significant and thus

shorten the lifetime.

Fig. 8 also shows the change in Tm^{3+} $^3F_4$ lifetime between the various bulk germanates discussed previously and the final fibre. These $^3F_4$ lifetimes are all greater than the Tm^{3+} $^3F_4$ lifetime in silica based fibres where 20μsec has been reported [29]. A further lengthening of the $^3F_4$ lifetime is also observed from pure germanate to lead-germanate glasses consistent with the lower frequency shift in the maximum phonon energy. For some applications, such as the diode pumped 2 μm thulium laser [30], it is important that decay from the $^3F_4$ level does not become totally dominated by radiative processes to the ground state, since multiphonon emission from the $^3F_4$ level, via $^3H_5$ level, is used to feed the $^3H_4$ upper laser level when diode pumping at 790nm into the $^3F_4$ level. Taking the Tm^{3+} $^3F_4$ radiative lifetime as falling within the range measured in other glasses, namely 1.2-0.8msec [28,31], then the branching ratio for multiphonon emission from the $^3F_4$ can be estimated for GPBZK glass to be in the range 60-80%.

Shortening of the $^3F_4$ lifetime from bulk GPBZK to fibre can be seen in Fig. 8, although the effect is less than that observed for the $^3H_4$ level. The reduction in the fraction the $^3F_4$ lifetime has been shortened in comparison to its original bulk value, is because all other decay processes present in the fibre must compete, in the case of the $^3F_4$ level, against much faster radiative and multiphonon relaxation processes. While, in the $^3H_4$ level the multiphonon processes are negligible and the radiative decay rate is higher, so any other decay processes will have a more significant effect (such as energy transfer etc.).

The $^1G_4$ lifetimes also show in Fig. 8 for the various germanate glasses discussed previously. The $^1G_4$ level is separated from the next lowest lying energy level by an energy gap of more than 6000 cm^{-1} making multiphonon emission from the $^1G_4$ level negligible even in silicate-type glasses [26]. Therefore the observed lifetime of the $^1G_4$ level can be taken as almost purely radiative for all glasses studied here, and comparisons of the $^1G_4$ lifetime between glasses can then be used to compare host dependent changes in the radiative decay process. And therefore their lifetimes are the good indicator of the structrual changes in thses glasses.

It was expected that the radiative lifetime of the germanates would be inversely proportional to the refractive index of the glasses through the local field correction factor in the Einstein A coefficient[33]. Between pure germanate and PbO-CaO-GeO_2 glass this axiom is confirmed, with the $^1G_4$ lifetime reduced in the lead germanate glass which has a much higher refractive index than pure germanate [8]. However, the $^1G_4$ lifetime

for the other lead-germanate glasses is longer than pure germanate, as can be seen in Fig. 8, despite the refractive index being higher in all the lead germanates, attaining a value of 1.812 in GPBZK glass. We attribute this to the structrual changes, especially the local structrual environments around the Tm^{3+}, from one composition to another. As the composition changing from GeO_2-PbO-CaO, GeO_2-PbO-CaO-Al_2O_3 to GeO_2-PbO-BaO-ZnO-K_2O, the narrower fluorescent emissions are observed (for more detail see the following section). This indicates the more defined local structures around the Tm^{3+} ions as the composition goes through the above series. According to Judd-Ofelt theory [26], the more regular the rare-earth sites, the less are the electric dipole transition strengths. Thus, the A values are lower and the lifetimes are longer.

Fluorescence Spectra

Presented in Fig. 9 are the visible fluorescence spectra from 600-900nm for all the thulium doped glasses discussed previously, the upper and lower halves of each spectrum are scaled separately. The electronic transitions giving rise to each of fluorescence bands are also shown in Fig. 9. The insert above the spectra in Fig. 9 shows the peak positions of the sharp fluorescence lines below 750nmm and a band is shown representing the full width at half maximum of the broad 790nm peak.

Comparison of the fluorescence spectra for lead-germanates with the fluorescence spectra for pure GeO_2, given as the lowest spectrum in Fig. 9 clearly shows a distinct narrowing and shift of the inhomogeneously broadened thulium spectrum in the lead-germanates. The narrowing of the inhomogeneous profile indicates a smaller variation in the thulium site in the lead germanates, which reflects the more stable glass forming characteristics of the lead-germanates.

Study of Fig. 9 shows there is less change in the spectra as different components are added to the lead-germanate, than when comparing the lead-germanate to the pure germanate. This confirms the dominant effect of lead on the glass structure as was previously indicated by the Raman spectra. The visible fluorescence spectra for the various different thulium doped lead-germanate compositions, shown in the mid part of Fig. 9, exhibit only a little change as additional glass components are added. In particular no significant spectral shifts are observed on the addition of alumina. This is in distinct contrast to thulium doped silica were large changes occur in the fluorescence properties of thulium doped aluminosilicates when compared to pure silica or germanosilicate hosts [29]. As was discussed previously in silica it is the alumina that acts

to create a more stable glass giving the observed spectral shifts. In the case of the modified lead-germanates it is clear that alumina has very little effect on the glass network. This echoes the conclusions of the thermal analyses of the bulk lead-germanate glasses discussed previously, where addition of alumina had little effect on the glass properties of the melt and agrees with the Raman spectra where no notable change was seen in the vibrational spectra on addition of alumina.

The slight peak narrowing observable in Fig. 9 between the fluorescence spectra for CaO-PbO-GeO_2 or CaO-PbO-Al_2O_3-GeO_2 and PbO-K_2O_3-BaO-ZnO-GeO_2 (GPBZK), indicates an even smaller variation of the thulium site in the GPBZK glass than other lead-germanate. This is in accord with the excellent glass forming abilities of the GPBZK glass and supports the greater effect ZnO has on stabilising the glass. No significant spectral changes are seen in the fibre when compared to the bulk GPBZK glass. The change in the form of the 790nm peak in the fibre is attributed to a change in the proportions of $^3F_4$-$^3H_6$ and $^1G_4$-$^3H_5$ fluorescence making up this emission band due to much higher light excitation intensities in the fibre.

The infrared emission spectra from 1.3-2.3μm for the thulium doped GPBZK glass fibre is presented in Fig. 10. Florescence from both the $^3H_4$-$^3H_6$ and $^3F_4$-$^3H_4$ transition is observed in the infrared spectrum. The fluorescence intensity of the $^3H_4$-$^3H_6$ transition shows less than a 6% variation over a 100nm range at the peak of the emission. It should therefore be possible to achieve a large, flat tuning curve when lasing this transition.

Lasing results

Initial lasing results for the $^3H_4$-$^3H_6$ transition at around 1.9μm in the GPBZK fibre have been reported by the same authors [6]. The minimum reported threshold was 3.6mW of launched light from 790nm diode using just 3cm of fibre. This compares to thresholds of 50mw in ZBLAN and 4.4 mW in alumina silica [30]. The best slope efficiency of the GPBZK laser was 13% from a cavity utilising Fresnel reflection from a bare fibre end to provide lasing feedback and act as a 90% output coupler. The best slope efficiency for silica fibre has been reported as 17% and 8.3% has been reported for Tm^{3+}:ZBLAN fibre (simultaneously lasing at 1.48μm). The lasing results for Tm^{3+}:GPBZK fibre therefore demonstrate considerable gains in threshold over previous demonstrations of lasing on the Tm^{3+} $^3H_4$-$^3H_6$ transition. Further improvements are anticipated with the optimisation of the fibre length used in the fibre cavities.

6. Conclusion

We have present an extension of fibre technology into a new rare-earth doped lower phonon-energy lead-germanate glass. This is achieved by optimizing the glass suitable for fibre-optic applications via the use, for the first time to our knowledge, of the Levin-Block concept. Absorption and emmission spectra, together with fluorescent decay times for the Tm^{3+} ions in the glass and fibre are discussed. The reduced maximum phonon-energy of lead-germanates ($890cm^{-1}$) over that of silicates ($1150cm^{-1}$) leads to an extension of the metastable lifetimes in Tm^{3+}. The important role of Pb^{2+} in influencing the glass structures and properties is addressed. Improvements in fibre device performance that have resulted from one particular thulium laser transition at around $2\mu m$ have already been reported [6]. Full utilisation of this new class of glass fibres is expected to lead to wealth of both new and improved devices.

Reference

1 :P. Urquhart, IEE Proc. 135(6), Pt. J, (1988) 385-407.

2 :E.M. Levin, S. Block, J. Am. Ceram. Soc., 40 (1957) 95-106, 113-118.

3 :E.M. Levin, S. Block, J. Am. Ceram. Soc., 41(2) (1958) 49-54.

4 :E.M. Levin, S. Block, J. Am. Ceram. Soc., 50(1) (1967) 29-38.

5 :A. Tropper, R. Smart, I. Perry, D. Hanna, J.R. Lincoln, W.S. Brocklesby, Proc. SPIE., 1373 (1990) p.152-157.

6 :J.R. Lincoln, C.J. Mackechnie, J. Wang, W.S. Broscklesby, R.S. Deol, A. Pearson, D.C.Hanna, D.N. Payne, Electron. Lett. 11 1992 1021-1022.

7 :W.H. Dumbaugh, Proc. SPIE, 297 (1981) 80-85.

8 :W.H. Dumbaugh, Opt. Eng., 24(2) (1985) 257-262.

9 :D.L. Wood, K. Nassau, D.L. Chadwick, Appl. Opt., 21(23) (1982) 4276-4279.

10 :A.F. Fray, S. Nielsen, Infrared Phys., 1 (1961) 175-186.

11 :J. Zarzycki, "Glasses and the Vitreous State", Cambridge University Press, 1991, p.68.

12 :N.J. Kreidl, In "Glass Science and Technology" 1, Chapt. 3, ed. by D.R. Uhlmann and N.J. Kreidl, Academic Press, New York and London, 1983, p.183.

13 :E.M. Levin, In "Phase diagram: Material Science and Technology", 3, ed. by A.M. Alper, Academic Press, New York and London, 1970, p.144-236.

14 :J. Zarzycki, "Glasses and Vitreous State", Cambridge University Press, 1991, p.155.

15 :W. Eitel, "Silicate Science", 2, Academic Press, New York and London, 1965, p.206.

16 :F.X. Gan, "Calculation of Physical Properties and Composition Design for Inorganic Glasses", Shanghai Science Press, Shanghai, 1981.

17 :B. Phillips, M.G. Schroger, J. Am. Ceram. Soc., 48(8) (1965) 398-401.

18 :P.W. France, S.F. Carter, M.W. Moore, C.R. Day, Br. Telecom. Technol. J., 5(2) (1987) 28-44.

19 :E.R. Taylor, D.J. Taylor, L. Li, M. Tachibana, J.E. Townsend, J. Wang, P.J. Wells, L.Reekie, P.R. Morkel, D.N. Payne, Mater. Res. Soc. Symp. Proc., 172 (1990) 321-327.

20 :N.P. Bansal, R.H. Doremus, "Handbook of Glass Properties", Academic Press, New York and London, 1986, p.223-227.

21 :A. Paul, "Chemistry of Glasses", Chapman and Hall Ltd., London and New York, 1982, p.76-85.

22 :J.H. Dickson, "Optical Instruments and Teckniques", Oriel Press, London, 1969.

23 :G. Orcel, D. Biswas, M.R. Shahriari, T. Iqbal, G.H.Siegel, Proc. 6th Inter. Symp. Halide Glasses., Clausthal-Zellerfeld, F.R. Germany, 1989, p.539-544.

24 : F.L. Galeener, G. Lucovsky; Phys. Rev. Lett. **37(22)** (1976) 1474-1478

25 :H.Hagiwara, R.Oyamada, J. Phys Soc. Japan **36(2)** (1974) 517-522

26 :R. Reisfeld and C.K. Jorgensen, in "Handbook on the physics and chemistry of rare-earths", ed. by K.A. Gschneidner, Jr. and L. Eyring, (Elsevier Science Publishers B.V., 1987), Chapter 58, pp. 1-90.

27 :S.Hufner, Optical Spectra of Transparent Rare Earth Compounds, Academic Press, New York, 1978

28 :E.W.J.l. Oomen; J. Lumin. **50** (1992) 317-332

29 :J.R.Lincoln, W.S.Brocklesby, F.Cusso, J.E.Townsend, A.C.Tropper, A.Pearson, J. Lumin. **50** (1991) 297-308

30 :W.L.Barnes, J.E.Townsend (J.R.Lincoln), Elec. Lett. **26(11)** (1990) 746-747

31 :R.Reisfeld, L.Boehm, N.Spector, Chem. Phys. Lett. **49(2)** (1977) 251-254

32 : G. Blasse; "Spectroscopy of Solid State Laser-Type Materials"ed B. DiBartolo (Plenum, New York. 1987) 199

33 :W.M. Yen "Laser Spectroscopy of Solids" eds W.M. Yen, P.M. Selzer (Springer, Berlin. 1981) 3

Fig. 1

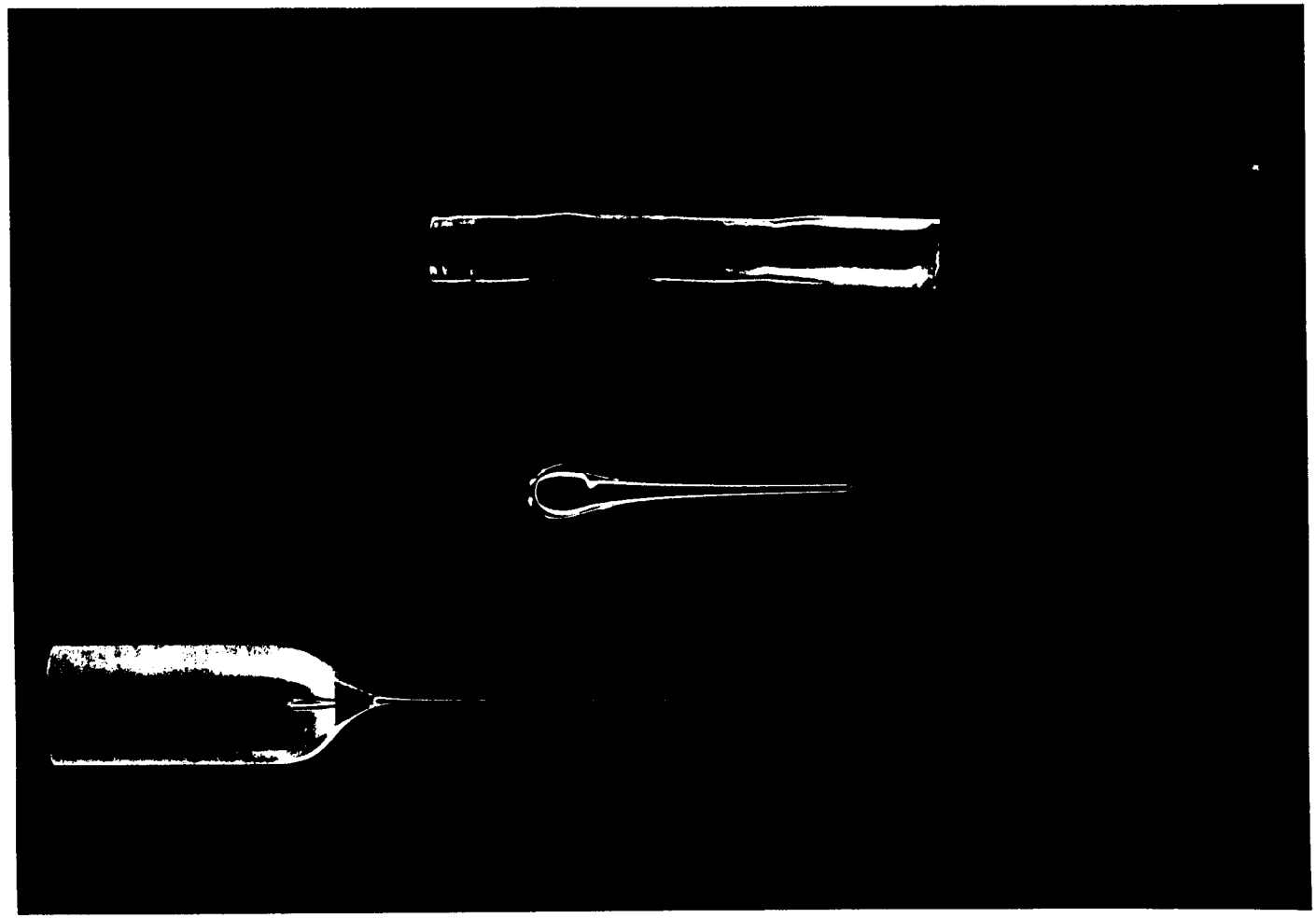

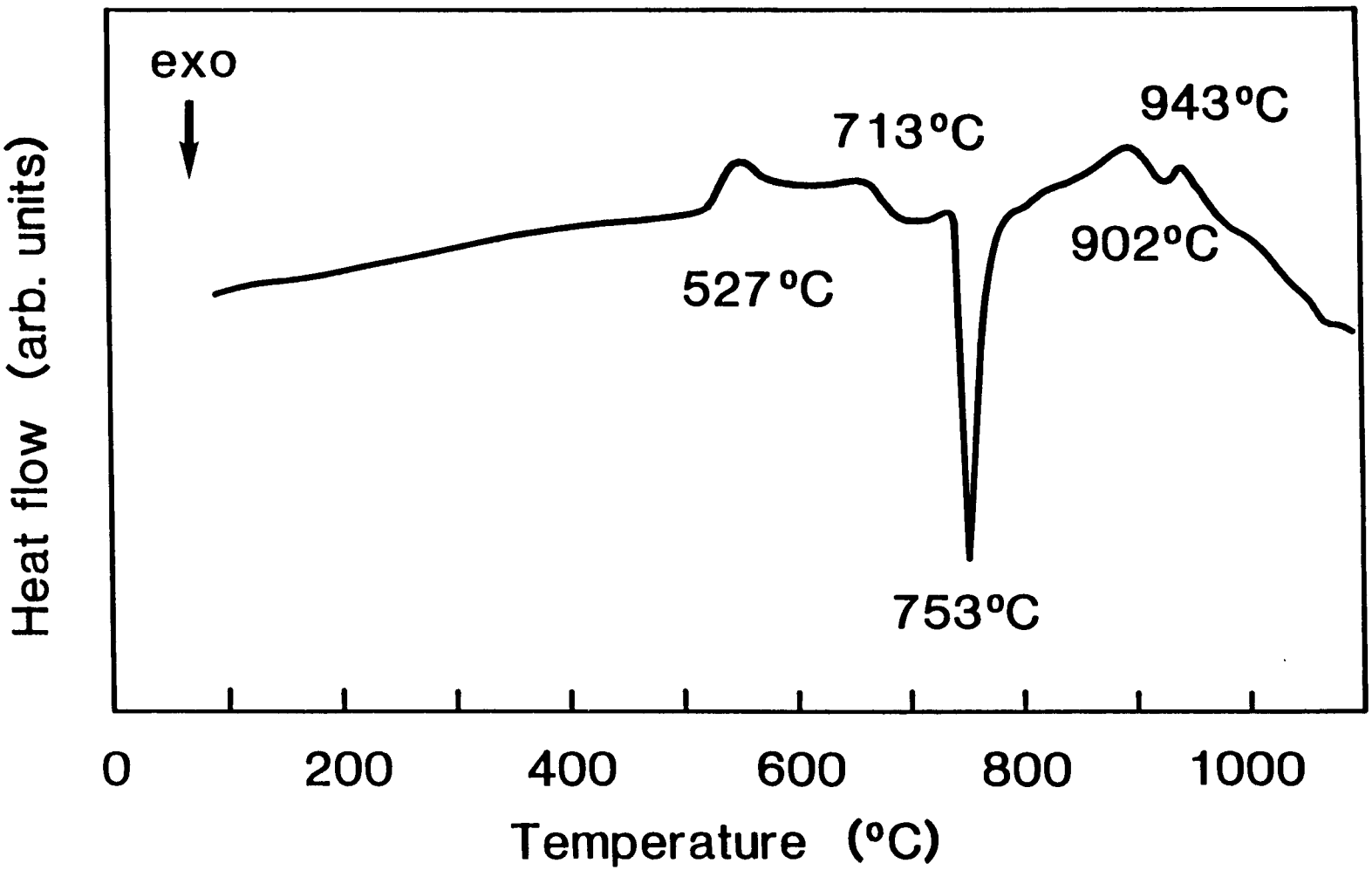
exo
713°C
943°C
902°C
527°C
753°C
Heat flow (arb. units)
0
200
400
600
800
1000
Temperature (°C)

Fig 2

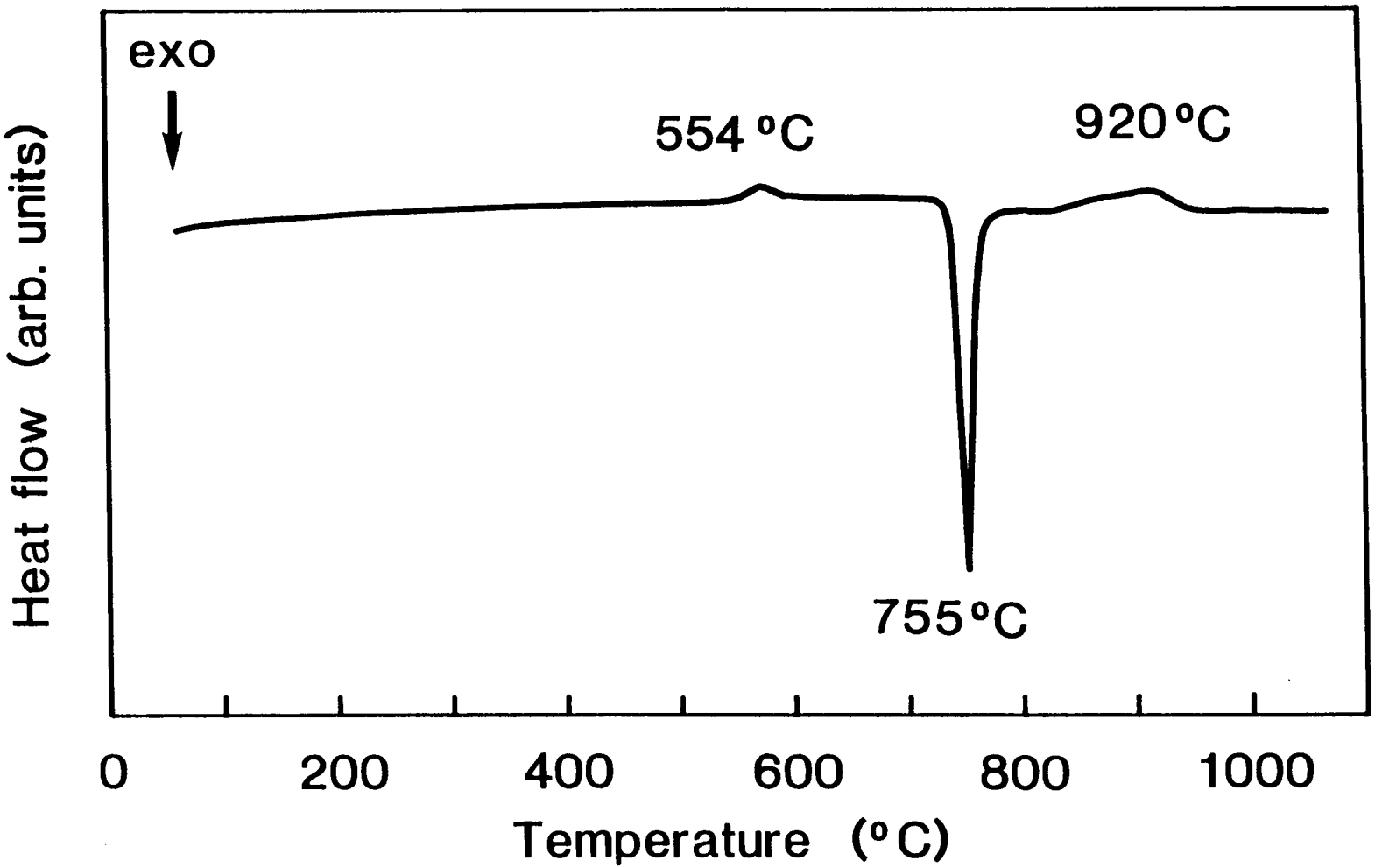
exo
554 °C
920 °C
755 °C
Heat flow (arb. units)
0
200
400
600
800
1000
Temperature (°C)

Fig. 3

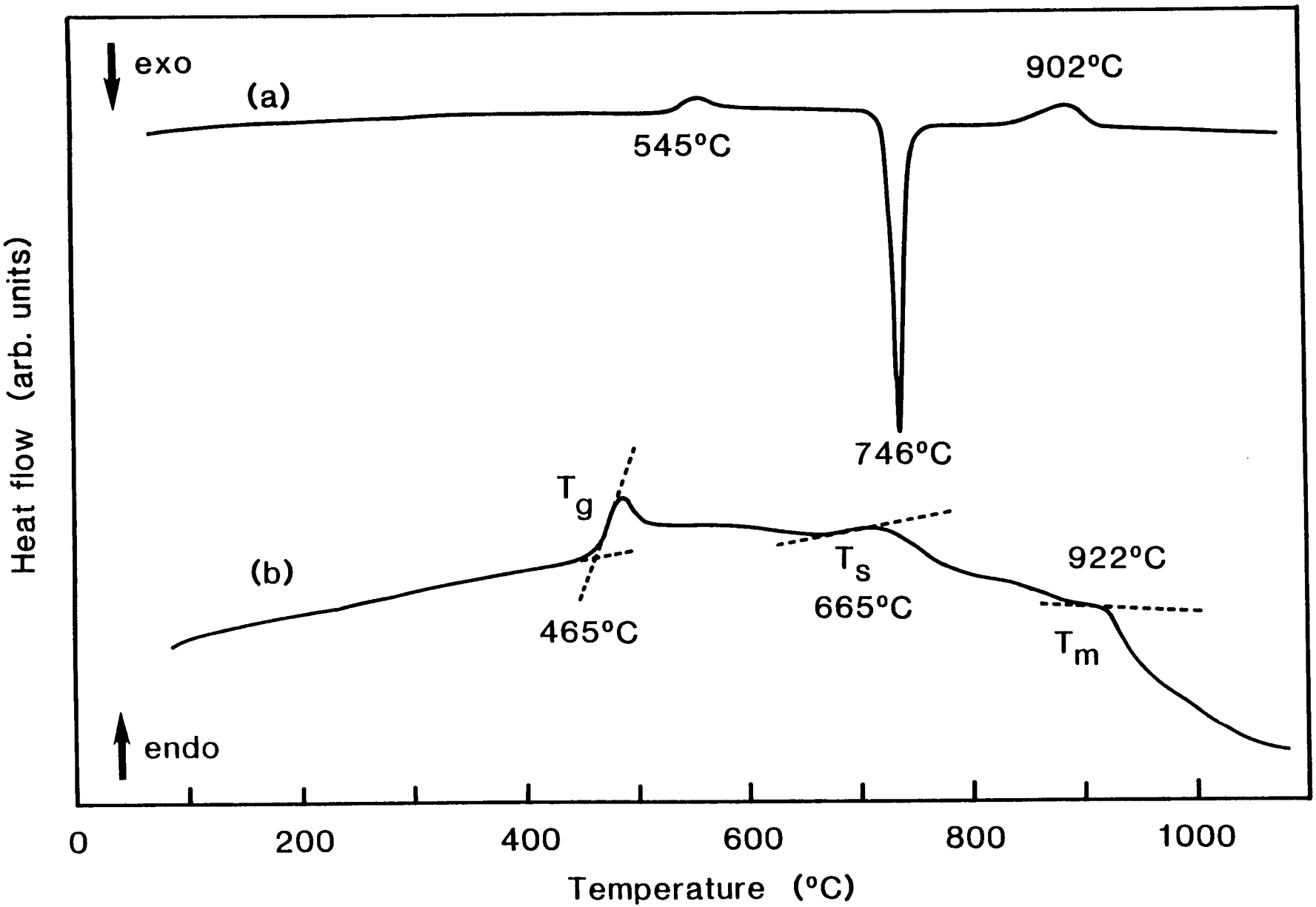
exo
(a)
902°C
545°C
746°C
Tg
(b)
Ts
665°C
922°C
465°C
Tm
endo
Heat flow (arb. units)
0
200
400
600
800
1000
Temperature (°C)

Fig. 4

UP
SUPERSURE
OBEN
UP
SUPERSURE
OBEN

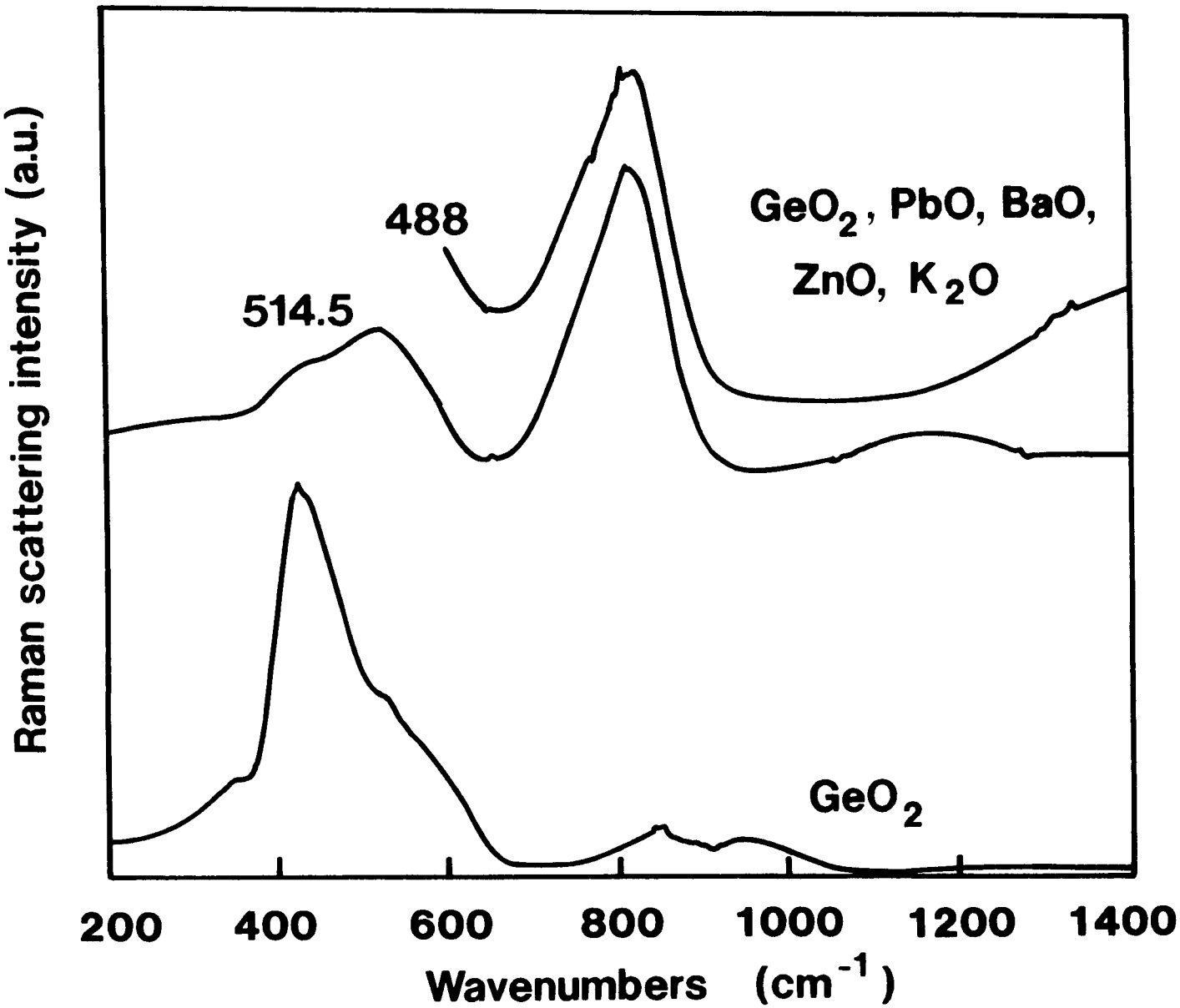
Raman scattering intensity (a.u.)
488
514.5
GeO_2, PbO, BaO,
ZnO, K_2O
GeO_2
200
400
600
800
1000
1200
1400
Wavenumbers (cm^{-1})

Fig 6

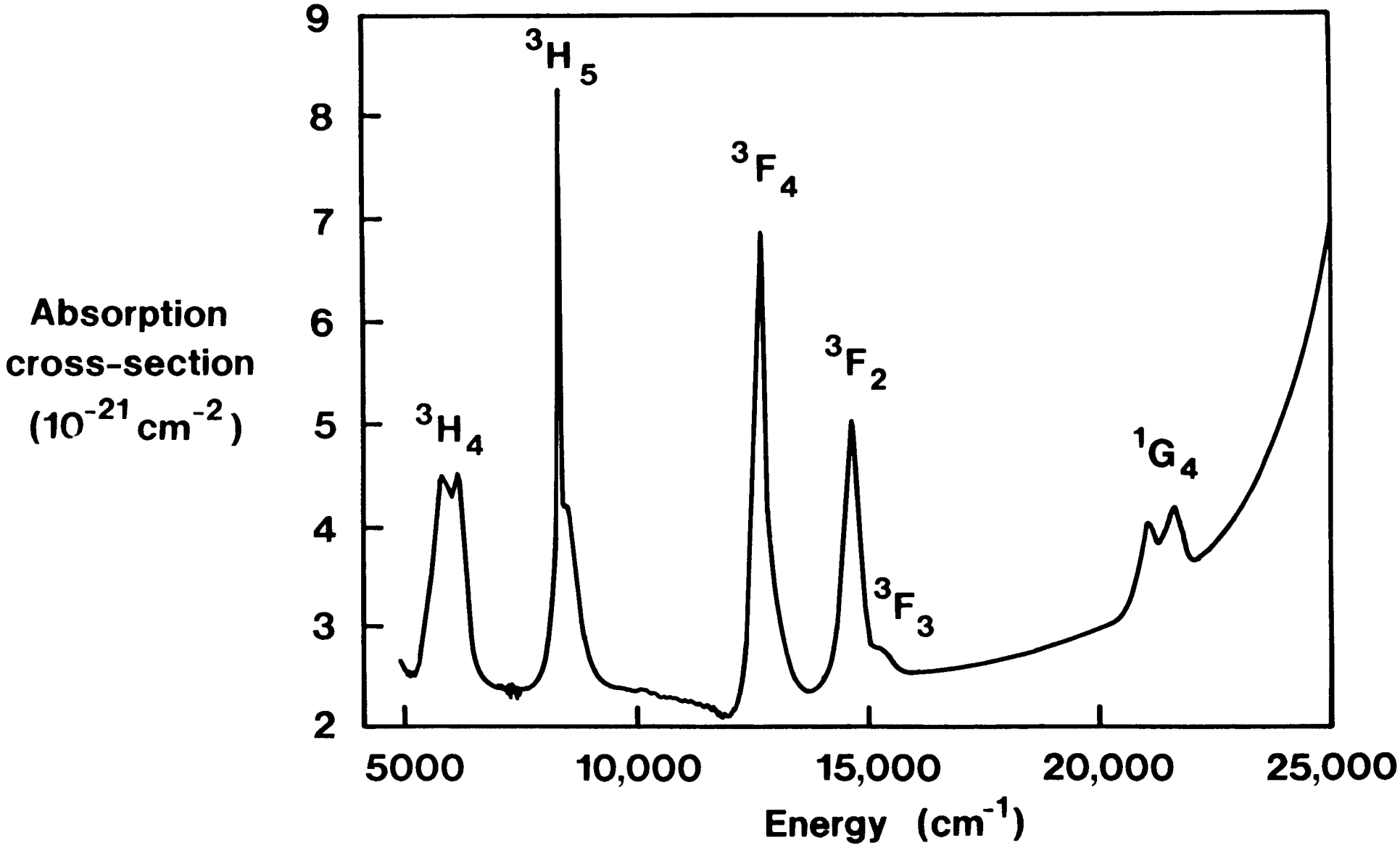
Absorption cross-section (10^{-21} cm^{-2})
9
8
7
6
5
4
3
2
$^3H_5$
$^3F_4$
$^3F_2$
$^3H_4$
$^3F_3$
$^1G_4$
5000
10,000
15,000
20,000
25,000
Energy (cm^{-1})

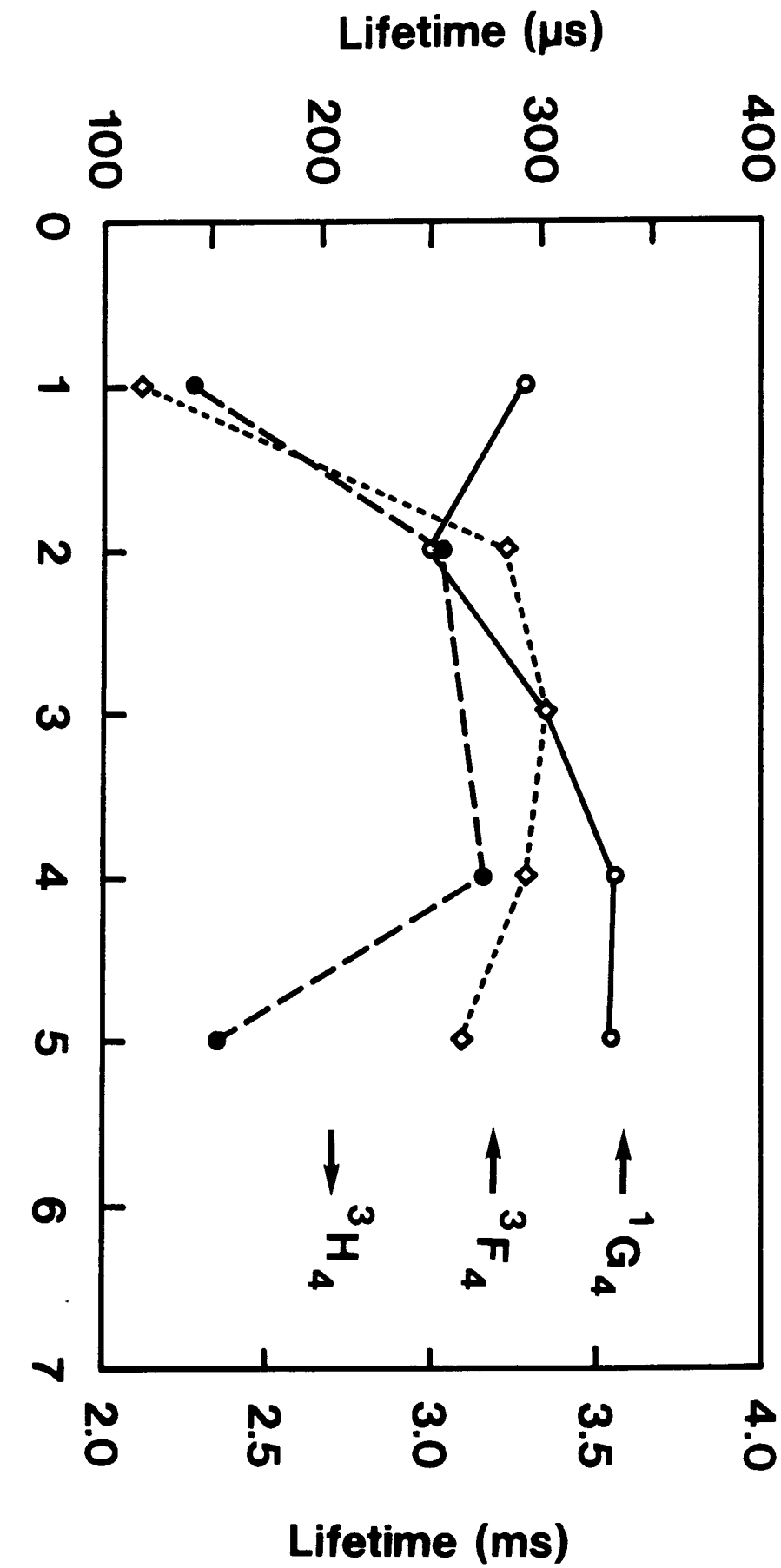
Lifetime (μs)
100
200
300
400
0
1
2
3
4
5
6
7
$^3H_4$
$^3F_4$
$^1G_4$
2.0
2.5
3.0
3.5
4.0
Lifetime (ms)

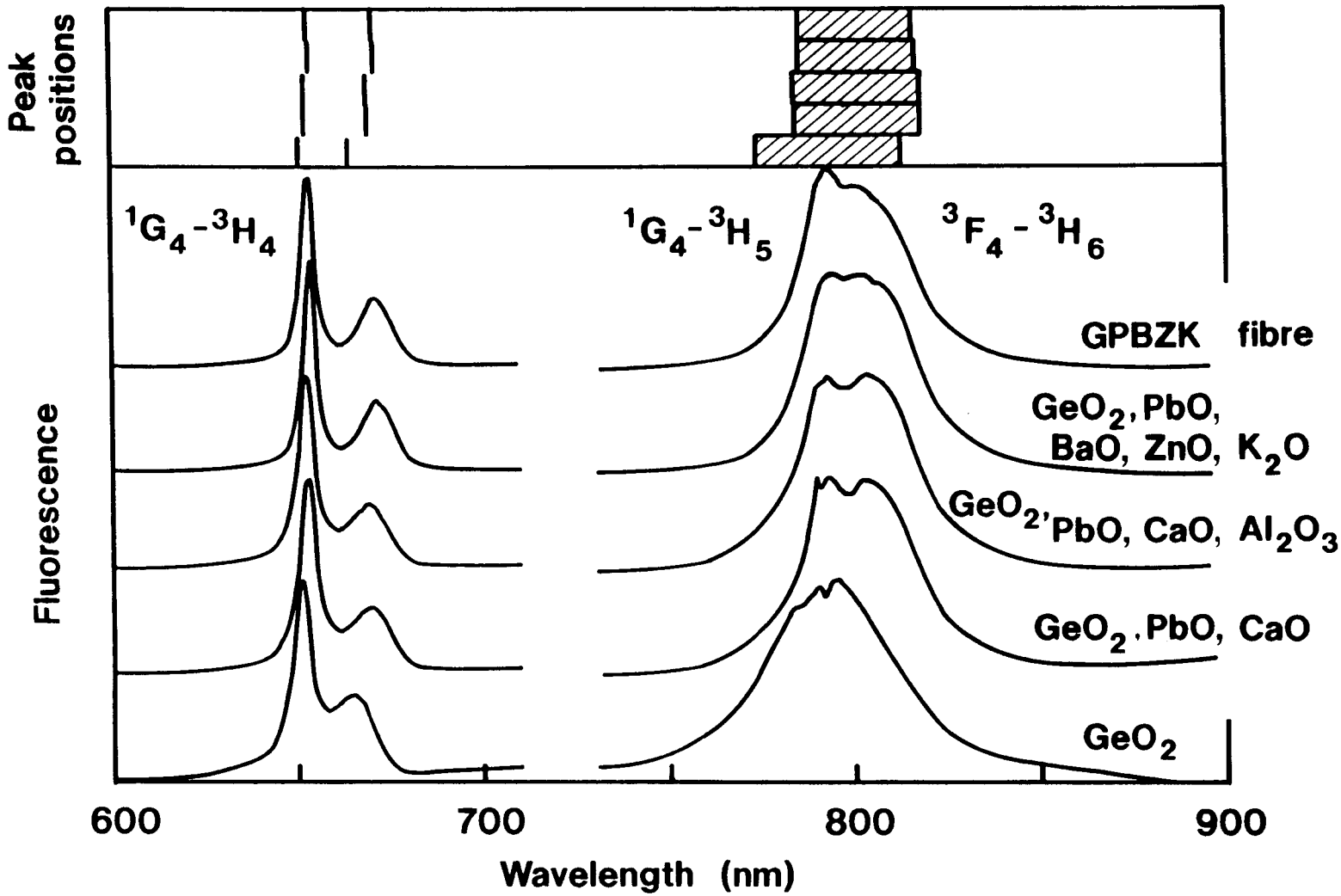
Peak positions
$^1G_4$-$^3H_4$
$^1G_4$-$^3H_5$
$^3F_4$-$^3H_6$
GPBZK fibre
GeO_2, PbO, BaO, ZnO, K_2O
GeO_2, PbO, CaO, Al_2O_3
GeO_2, PbO, CaO
GeO_2
Fluorescence
600
700
800
900
Wavelength (nm)

Fig. 9

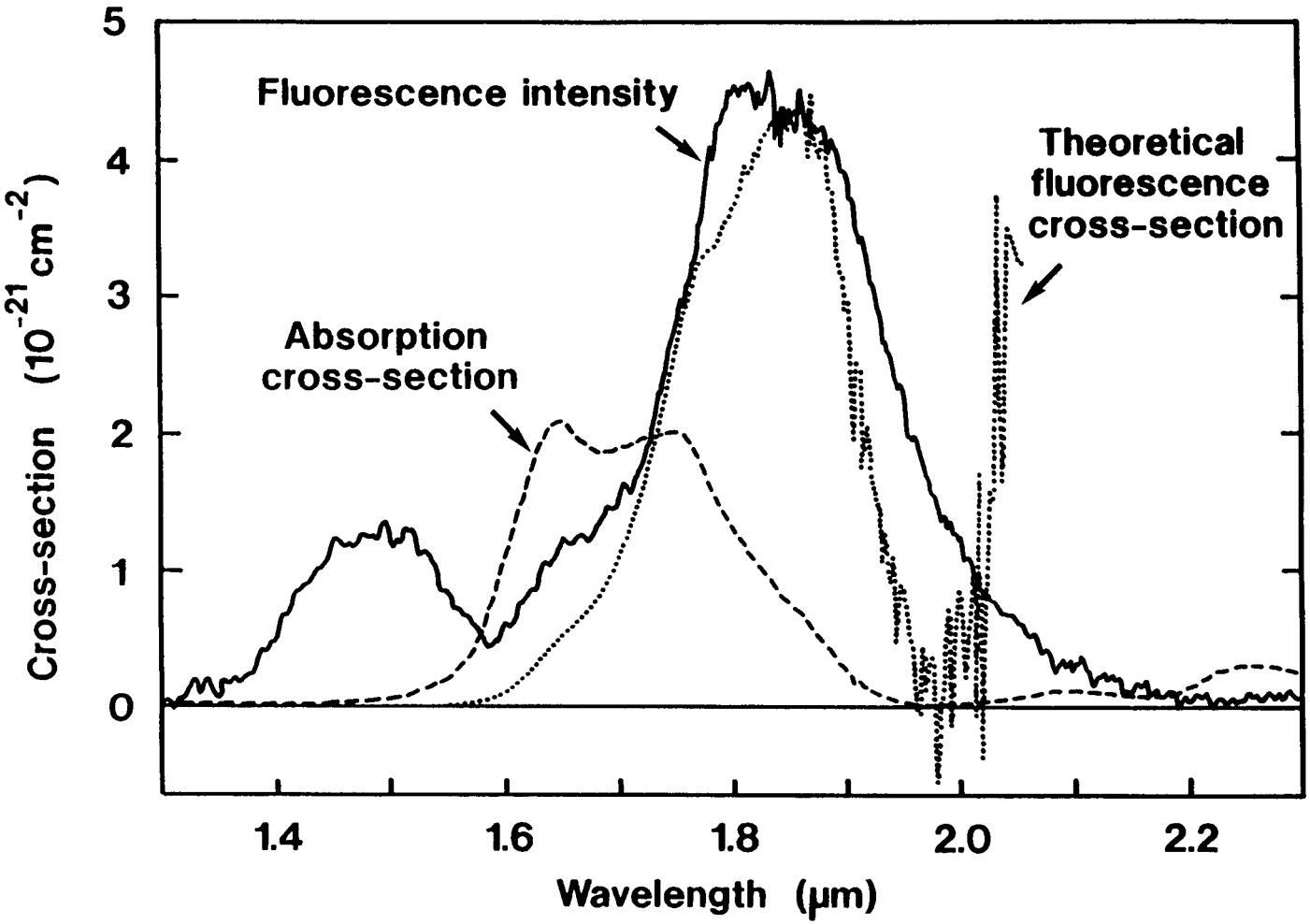
Fluorescence intensity
Theoretical
fluorescence
cross-section
Absorption
cross-section
Cross-section (10^{-21} cm^{-2})
5
4
3
2
1
0
1.4
1.6
1.8
2.0
2.2
Wavelength (μm)